Springer

KSME

Journal of Mechanical Science and Technology 31 (1) (2017) 99~109
www.springerlink.com/content/1738-494x(Print)/1976-3824(Online)
DOI 10.1007/s12206-016-1210-6

Multiscale singular value manifold for rotating machinery fault diagnosis †

Yi Feng, Baochun Lu* and Dengfeng Zhang

School of Mechanical Engineering, Nanjing University of Science and Technology, Nanjing, 210094, China

(Manuscript Received April 4, 2016; Revised July 10, 2016; Accepted August 17, 2016)

Abstract

Time-frequency distribution of vibration signal can be considered as an image that contains more information than signal in time domain. Manifold learning is a novel theory for image recognition that can be also applied to rotating machinery fault pattern recognition based on time-frequency distributions. However, the vibration signal of rotating machinery in fault condition contains cyclical transient impulses with different phrases which are detrimental to image recognition for time-frequency distribution. To eliminate the effects of phase differences and extract the inherent features of time-frequency distributions, a multiscale singular value manifold method is proposed. The obtained low-dimensional multiscale singular value manifold features can reveal the differences of different fault patterns and they are applicable to classification and diagnosis. Experimental verification proves that the performance of the proposed method is superior in rotating machinery fault diagnosis.

Keywords: Rotating machinery; Fault diagnosis; Multiscale singular value; Manifold learning

1. Introduction

Vibration signals of rotating machinery in fault condition contain complex components which are diverse in both time and frequency domains. For non-stationary and nonlinear fault signal, neither isolated time domain nor frequency domain features can comprehensively represent the signal characteristics [1]. Time-frequency distribution (TFD) is prominent in establishing the comprehensive relationship between time and frequency domains [2]. The non-stationary and nonlinear features of signal revealed by TFD can effectively reflect the operating status of rotating machinery.

Manifold learning [3, 4] is mainly applied in the field of image recognition [5, 6], which can reduce the dimension of nonlinear and high-dimensional data and reveal the potential features of data structure. Some global nonlinear dimensionality reduction algorithms based on manifold learning have been proposed, such as isometric mapping (Isomap) [3], Locally linear embedding (LLE) [4] and Local tangent space alignment (LTSA) [7, 8]. In the field of rotating machinery fault diagnosis, Wang [9] applied manifold learning to extract the impulse features from multiscale envelope signal; He [10] applied manifold learning to extend the duration of the impact features. Su and Gan [11, 12] constructed compound manifold features for multi-fault diagnosis. Previous studies show that manifold learning can reflect the differences of signal characteristics of rotating machinery in different operating status.

In fact, the TFDs of vibration signals can be also considered as images. Therefore, rotating machinery fault diagnosis is achievable through recognizing the TFD images of vibration signals with the application of manifold learning.

An image with 100×100 pixels can be considered as a point in 10000-dimension space. Having similar images means the corresponding points are close to each other in the space. However, the phases of cyclical transient impulses and rotating frequency modulation are different in each signal sample, the corresponding points of TFD images from a same pattern are dispersedly distributed on a manifold structure in high-dimensional space. Therefore, when several similar fault patterns happen, manifold structures of different fault patterns might cross each other in the space and the sample points in mixing zone are hard to recognize, as shown in Fig. 1.

In this study, a Multiscale singular value manifold (MSVM)

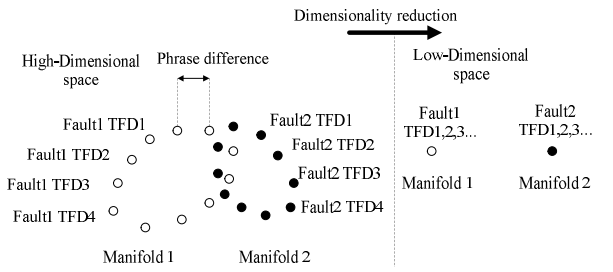

Fig. 1. TFD points in space.

*Corresponding author. Tel.: +86 13815854007, Fax.: +86 84315612
E-mail address: lbcnust@sina.com
† Recommended by Associate Editor Byeng Dong Youn

method was proposed to eliminate the effects of phase differences and extract the inherent features of TFDs. Through reducing the dimension of TFDs, outstanding sample clustering results and diagnosis effects can be obtained. All applied methods in MSVM, such as continuous wavelet transform, phase space reconstruction and singular value decomposition are proven and effective techniques, which makes fault diagnosis approach convenient and efficient.

2. Multiscale singular value manifold method

2.1 TFD based on continuous wavelet transforms

Time-frequency distribution is an effective tool to represent the features of multi-component signal in both time and frequency domains, which reveals more features than isolated frequency or time domain signal [1, 2]. The TFD based on EMD and Hilbert–Huang Spectrum [13] is interfered by end effect, the time series length of TFD based on short-time Fourier transform is shorter than the original signal [10]. Compared to those methods, the performance of Continuous wavelet transform (CWT) is superior in time-frequency analysis.

For signal *x(t)* continuous wavelet transform can be expressed as [14]:

$$wt(a,u)=\frac{1}{\sqrt{a}}\int_{-\infty}^{+\infty}x(t)\psi^{*}(\frac{t-u}{a})dt\ , \tag{1}$$

where *wt(a,u)* is the wavelet coefficient of signal at time *t* with scale factor *a* and time shift factor *u*. ψ^{*} is the complex conjugate of wavelet function ψ in permit condition:

$$\int_{-\infty}^{+\infty}\psi(t)dt=0\ . \tag{2}$$

Complex Morlet wavelet is introduced since its waveform is similar to the transient impulse of rotating machinery fault signal [15]:

$$\psi(t)=\frac{1}{\sqrt{\pi f_b}}e^{-t^2/f_b}e^{i2\pi f_c t}\ , \tag{3}$$

where f_b and f_c are waveform parameters which determine the bandwidth and center frequency of the wavelet function. In this study the parameters are not focus points, and then they are set to be $f_b = 1.5$ and $f_c = 1$.

With complex Morlet wavelet, the TFD of signal can be expressed as:

$$E(a,u)=\sqrt{\left[\mathrm{Re}\left(wt(a,u)\right)\right]^2+\left[\mathrm{Im}\left(wt(a,u)\right)\right]^2}\ , \tag{4}$$

where *E(a,u)* is the envelope signal in scale *a* and at time *u*. $a \in [1, \lambda]$, λ is the total number of TFD scales, $u \in [1, N]$, *N* is the length of signal. The relationship between component frequency *f* of each scale and corresponding scale *a* is $f = af_s/2\lambda$ (f_s is sampling frequency). Accordingly, the TFD of signal can be considered as an image with $\lambda \times N$ pixels.

2.2 Phase space reconstruction

Phase space reconstruction (PSR) [16] can reconstruct the inherent dynamic features embedded in a time series. For a time series $x(t) = [x_1, x_2, \ldots, x_N]$ with embedding dimension *m* and time lag τ, the *i*-th phrase point vector can be expressed as:

$$X_i^m=[x_i, x_{i+\tau}, \cdots, x_{i+(m-1)\tau}]\ . \tag{5}$$

The appropriate embedding dimension m can be obtained according to Cao's method [17]. Based on Takens' theory [18], the highest analytical accuracy of time series can be achieved when the time lag τ is set to be 1. Then the phase space of *x(t)* can be reconstructed as:

$$\begin{bmatrix} X_1^m \\ X_2^m \\ \vdots \\ X_i^m \\ \vdots \\ X_n^m \end{bmatrix}=\begin{bmatrix} x_1 & x_2 & \cdots & x_m \\ x_2 & x_3 & \cdots & x_{m+1} \\ \cdots & \cdots & \cdots & \cdots \\ x_i & x_{i+1} & \cdots & x_{i+(m-1)} \\ \cdots & \cdots & \cdots & \cdots \\ x_n & x_{n+1} & \cdots & x_N \end{bmatrix}. \tag{6}$$

To reconstruct the inherent dynamic features in time and frequency domains, each scale of TFD is reconstructed according to Eq. (6). Hence, the reconstructed phase space of TFD (RTF) can be expressed as:

$$RTF=\left[E^m(1)\quad E^m(2)\quad \cdots\quad E^m(\lambda)\right]^T\ , \tag{7}$$

where *E(a)* is the envelope signal in scale *a*, $E^m(a)$ is the reconstructed phase space of *E(a)* with embedding dimension *m*.

2.3 Dimensionality reduction based on singular value decomposition and manifold learning

Singular value decomposition (SVD) [19] is a proven method for matrix inherent feature extraction and dimensionality reduction. A matrix $\mathbf{X}_{n\times m}$ can be decomposed into 1 diagonal matrix and 2 orthogonal matrixes by SVD method, which can be expressed as:

$$\mathbf{X}_{n\times m}=\mathbf{U}_{n\times n}\mathbf{S}_{n\times m}\mathbf{V}_{m\times m}^{T}\ , \tag{8}$$

where $\mathbf{S}_{n\times m}$ is the diagonal matrix with nonzero diagonal elements $sv_1, sv_2, \ldots, sv_m$ ($sv_1 \geq sv_2 \geq \ldots \geq sv_m > 0$, $m < n$), $\mathbf{U}_{n\times n}$ and $\mathbf{V}_{m\times m}$ are orthogonal matrixes. For fault signal samples, the diagonal element vector $sv = [sv_1, sv_2, \ldots, sv_m]$ can represent the inherent dynamic features of corresponding recon-

structed phase space matrixes in lower dimension and avoid the influences cause by phase differences.

Accordingly, the reconstructed phase space of TFD (RTF) can be decomposed by SVD in each scale, and then the low-dimensional time-frequency singular value matrix TFSV is obtained:

$$\mathrm{TFSV} = \left[sv(1) \quad sv(2) \quad \cdots \quad sv(\lambda) \right]^T . \tag{9}$$

Through PSR and SVD method, a $\lambda \times N$ TFD image of signal has been reduced to a $\lambda \times m$ TFSV matrix ($m < N$). To implement a further dimensionality reduction, the time-frequency singular value matrix of each signal sample is connected scale by scale and constructed to be a multiscale singular value vector, which can be expressed as:

$$msv = \left[sv_1(1) \quad \cdots \quad sv_m(1) \quad sv_1(2) \quad \cdots \quad sv_m(\lambda) \right]^T . \tag{10}$$

Manifold learning is a theory for global nonlinear dimensionality reduction, and LTSA [7] is an excellent dimensionality reduction algorithm based on manifold learning. For the multiscale singular value matrix $\mathrm{MSV}_{(\lambda\times m)\times L} = [msv_1, msv_2, \ldots, msv_L]$ of L signal samples ($msv_i \in R^{(\lambda\times m)}$), the feature dimension $\lambda \times m$ can be reduced to d ($d < \lambda \times m$) by LTSA algorithm, which can be expressed as follow steps [7]:

2.3.1 Extract local information

Select the k nearest neighborhoods of each msv_i (i = 1, 2, …, L) according to Euclidean distance to construct the local information matrix msv^k_i:

$$msv_i^k = [msv_{i1}, msv_{i2}, \ldots, msv_{ik}] . \tag{11}$$

Remove the mean of k nearest neighborhoods from the msv^k_i matrix, and then calculate the d largest right singular vectors of the centralized msv^k_i matrix to construct the local orthogonal basis V_i:

$$V_i = [g_1, g_2, \cdots, g_d] . \tag{12}$$

2.3.2 Construct alignment matrix

Determine the 0-1 selection matrix $\mathbf{S}_i$:

$$\mathbf{S}_i = \mathrm{MSV}^{-1}_{(\lambda\times m)\times L} msv_i . \tag{13}$$

Calculate the correlation matrix $\mathbf{W}_i$:

$$\mathbf{W}_i = I - \left[\frac{e_k}{\sqrt{k}} V_i \right] \left[\frac{e_k}{\sqrt{k}} V_i \right]^T , \tag{14}$$

where e_k is a column vector of k ones.

Construct the alignment matrix $\mathbf{B}$ as:

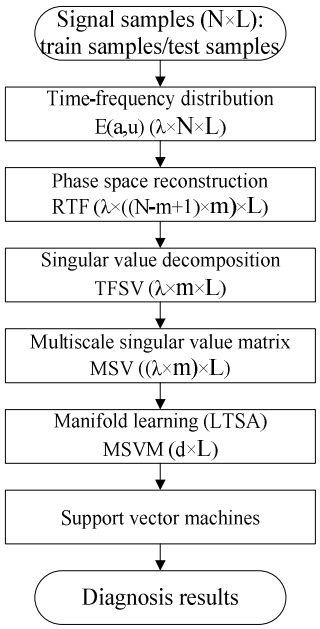

Fig. 2. MSVM fault diagnosis method.

$$\mathbf{B} = \sum_{i=1}^{i=L} \mathbf{S}_i \mathbf{W}_i \mathbf{W}_i^T \mathbf{S}_i^T . \tag{15}$$

2.3.3 Align global coordinates

Calculate the d+1 smallest eigenvectors of matrix $\mathbf{B}$, and then select the 2nd to the d+1-th smallest eigenvalues to constitute the global coordinates MSVM ($\in R^{d\times L}$). Accordingly, the d-dimension manifold features are obtained:

$$\mathrm{MSVM}_{d\times L} = \left[u_2 \quad u_3 \quad \cdots \quad u_{d+1} \right]^T , \tag{16}$$

where $u_{i+1} \in R^L$ (i = 1, 2, …, d) are corresponding to the i-th manifold features of L signal samples.

Through two steps of dimensionality reductions based on singular value decomposition and manifold learning, the high-dimensional TFDs of signal samples are reduced to lower dimension. The low-dimensional features are beneficial to sample classification and pattern recognition.

In summary, the multiscale singular value manifold method can be expressed as Fig. 2 and following steps:

(1) Divide signal samples from each class into train samples and test samples randomly with a determined ratio;

(2) Calculate the TFDs of signal samples with complex Morlet wavelet;

(3) Reconstruct the phase space of TFDs in each scale to obtain RTFs;

(4) Reduce the dimension of RTFs through SVD and extract inherent features of each scale as time-frequency singular value matrix TFSV;

(5) Construct the multiscale singular value matrix MSV of all samples;

(6) Reduce the dimension of MSV through manifold learn-

Table 1. Tested cases.

Cases	Sample classes	Samples (Each class)	
		Train	Test
Gearbox	3	30	20
Bearing 1	3	30	20
Bearing 2	4	30	20
Bearing 3	5	30	20

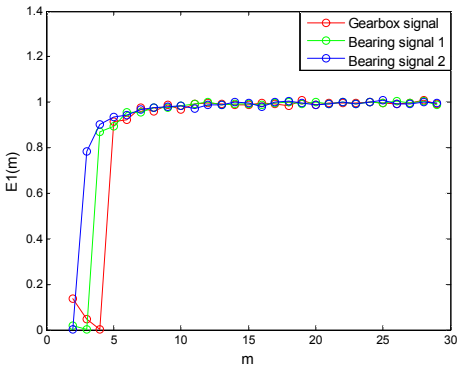

Fig. 3. Embedding dimension selection.

ing to obtain multiscale singular value manifold features MSVM;

(7) Train the Support vector machine (SVM) [20-22] with MSVM features of train samples and classify test samples with the trained SVM.

(8) Diagnose the fault patterns with clustering results and classification accuracies.

3. Experimental verification

Four cases are tested to verify the performance of proposed MSVM method. They are gear fault, bearing extended defect fault, bearing multiple fault positions and bearing multiple fault severities, as shown in Table 1. Several related methods are also applied to those cases as comparisons to the proposed method:

(1) SVDM: Without considering the frequency domain, signal samples in time domain are reconstructed in phase space and decomposed by SVD. Then we reduce the dimension of singular value vectors of all samples through manifold learning. The corresponding low-dimensional features are SVDMs.

(2) TFDM: The TFDs of signal samples are considered as images ($\lambda \times N$-dimension) and recognized by manifold learning. The corresponding low-dimensional features are TFDMs.

According to Cao's method, $E1(m)$ is defined to evaluate the robustness of embedding dimension m to noise [17]. Signals from Cases I, II and III are tested, as shown in Fig. 3. The trends of $E1(m)$ are stable when m is larger than 10. In this study, m is set to be 12, which means good robustness to noise. To obtain appropriate TFDs of all signal samples, the scale λ is set to be 128.

Table 2. Gear parameters.

Gear	Teeth	Rotating frequency (Hz)	Meshing frequency (Hz)
Drive	55	14.3	788
Driven	75	10.5	788

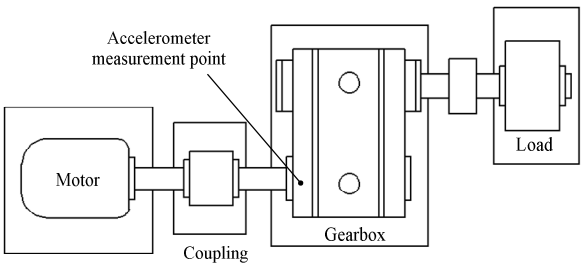

Fig. 4. Gearbox.

Case I: Gear fault

Vibration signal samples are acquired at the drive shaft side of the gearbox, as shown in Fig. 4. Normal gears and defective gears are respectively installed in the gearbox and the output shaft is coupled to load. In running status, vibration signal samples are acquired by accelerometer. The rotating frequency of motor is 14.3 Hz, the sampling frequency is 5120 Hz and the sampling time of each signal sample is 1 second. The signal sample classes are normal, driven gear with pitting defect and drive gear with wear defect. The parameters of gears are shown in Table 2. The TFD of each class is shown in Fig. 5.

The dimensionality reduction parameter d is set to be 2. As the low-dimensional features show in Figs. 6(a) and (b), the MSVM features of each class are very stable and samples from three classes are almost distributed at three points. As the clustering results of SVDM show in Fig. 6(c), some samples from normal and pitting defect are mixed and the samples from each class are distributed in lines. As the image recognition results of TFDM method shown in Fig. 6(d), the samples from each class are distributed quite close to the other classes and they cannot be distinguished or identified accurately.

Case II: Bearing extended defect fault

Experimental platform and bearings (HRB-1209) with different ranges of pitting defects are shown in Fig. 7. Pitting defects (depth 0–0.019 inch) are artificially machined on one side of the outer race surface. Normal bearing and defective bearings are respectively installed in the test end and the radial load is set in the middle of the shaft. In running status, vibration signal samples are acquired by accelerometers in both horizontal and vertical directions of the test end. The rotating frequency of motor is 15 Hz, the sampling frequency is 25600 Hz and the sampling time of each signal sample is 0.5 second. The defect parameters of outer race surface are shown in Table 3. The TFD of each signal class is shown in Fig. 8, within 0–0.1s time range.

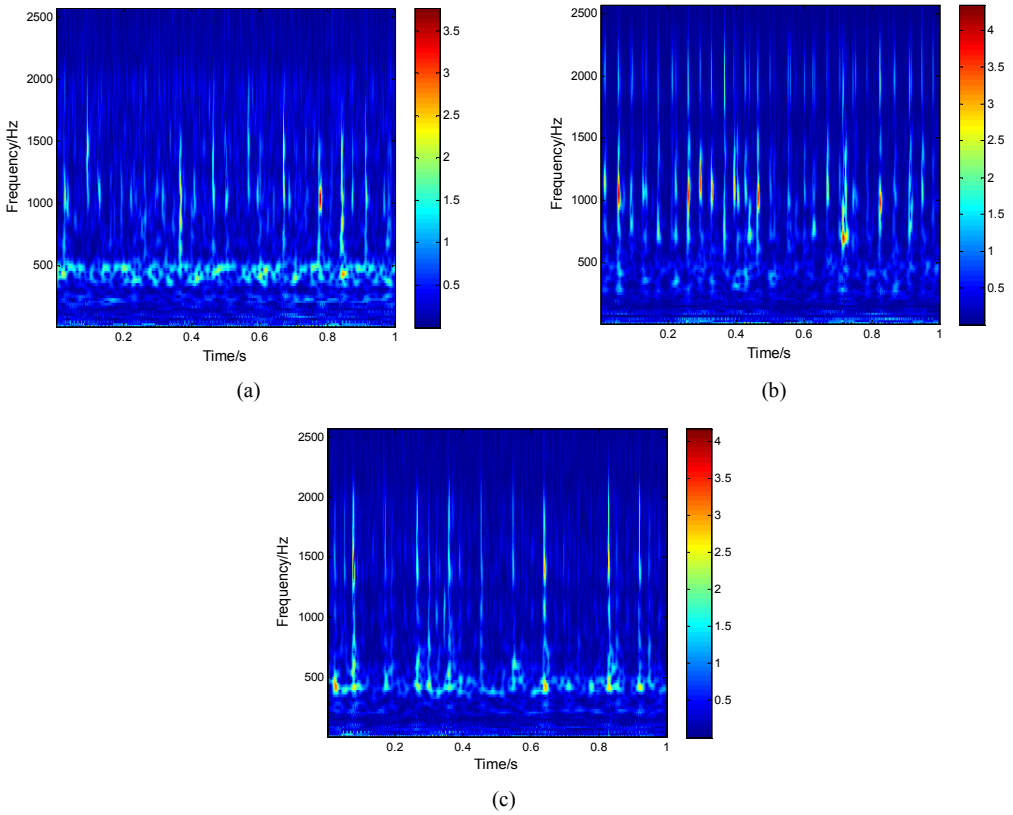

Fig. 5. Time-frequency distributions: (a) Normal; (b) wear; (c) pitting.

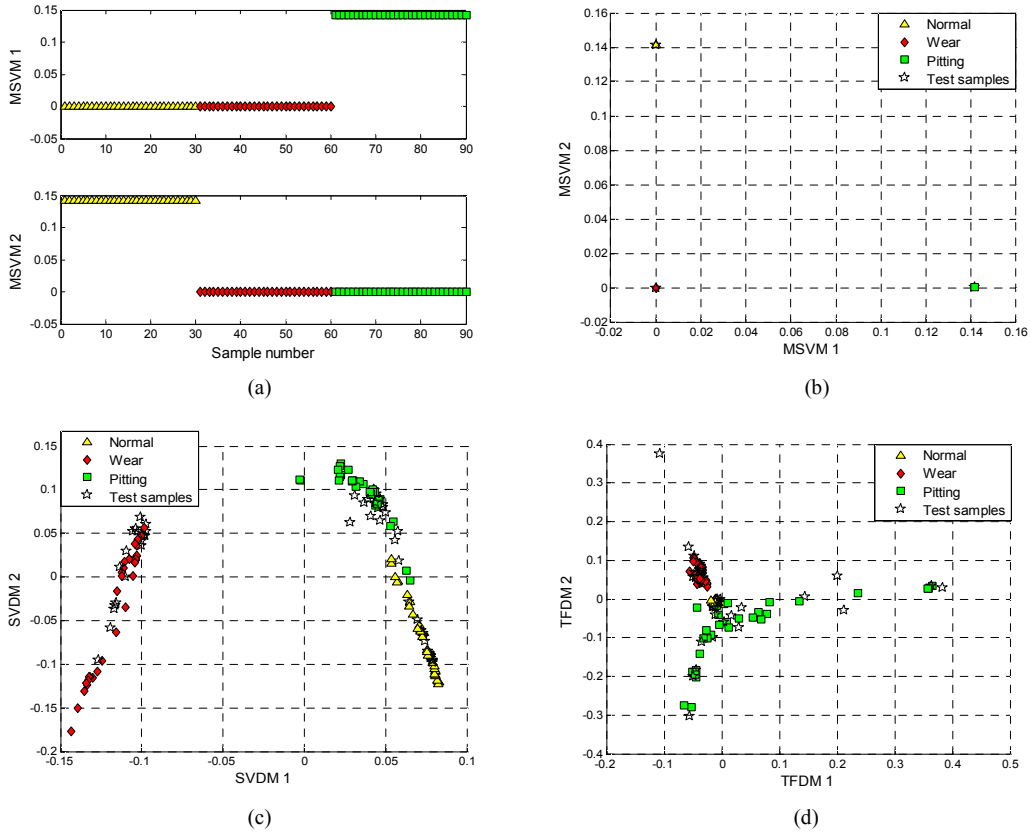

Fig. 6. Clustering results: (a) MSVM features; (b) MSVM; (c) SVDM; (d) TFDM.

Table 3. Parameters of bearings.

Defect type	Defective range	Fault frequency (Hz)
Normal	0	—
Local defect	$\pi/16$	102.5
Extended defect	$5\pi/16$	102.5

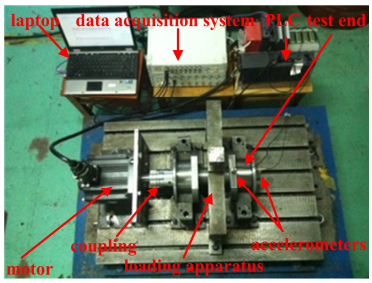

(a)

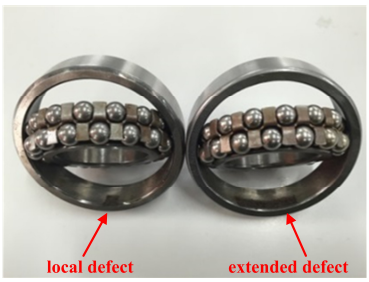

(b)

Fig. 7. Bearing experiment: (a) Experimental platform; (b) local defect and extended defect bearings.

The dimensionality reduction parameter d is set to be 2. As the low-dimensional features show in Figs. 9(a) and (b), the MSVM features of each class are very stable and samples from three classes are almost distributed at three points. As the clustering results of SVDM show in Fig. 9(c), normal signal samples are separated from the other samples, while the samples from local defect and extended defect are not completely distinguished, and some samples from two fault patterns are still mixed. As the image recognition results of TFDM method show in Fig. 9(d), normal signal samples are away from fault samples, while the samples from extended defect are almost surrounded by the samples from local defect. Hence, the samples from two fault patterns are too close to distinguish clearly.

Case III: Multiple fault positions

Bearing data is collected from the CWRU bearing data center [23]. The rotating frequency of drive shaft is 30 Hz, the sampling frequency is 12000 Hz, and the sampling time of each signal sample is 0.4 second. Signal samples are acquired from normal bearing (SKF-6205) and bearings with defects which are artificially machined on the surfaces of outer race, inner race and rolling element. The defect size is 0.007 inch. The corresponding fault feature frequencies of fault patterns are Ball passing frequency on outer race (BPFO) 107.3, Ball passing frequency on inner race (BPFI) 162.2 and Ball fault frequency (BFF) 141.5 Hz.

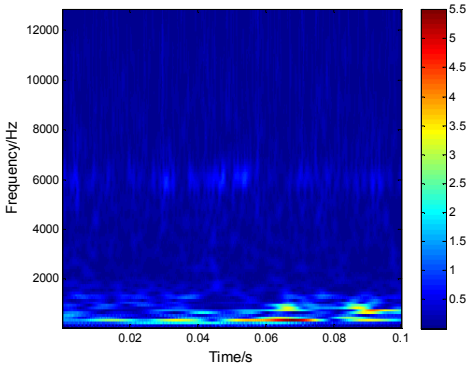

(a)

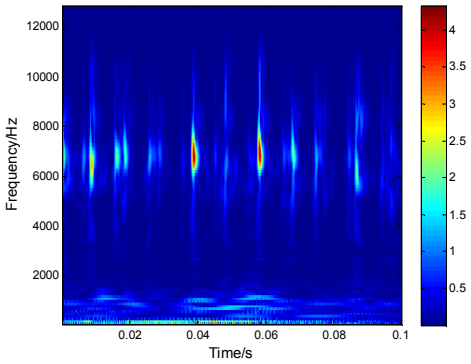

(b)

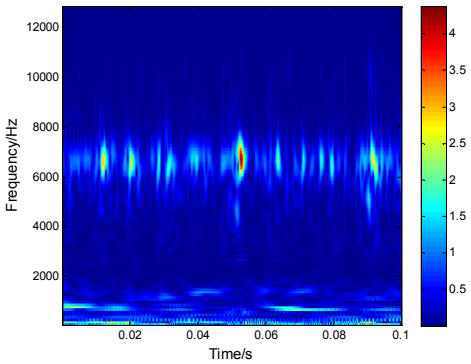

(c)

Fig. 8. Time-frequency distributions: (a) Normal; (b) local defect; (c) extended defect.

The dimensionality reduction parameter d is set to be 3. As the low-dimensional features and clustering results show in Figs. 10(a)-(c), all samples are almost distributed at four points and the sample concentrating effect of SVDM method is consistent with that of MSVM method. As the image recognition results of TFDM method show in Fig. 10(d), the samples from each class are separated from the other classes, while the samples from rolling element defect are close to the samples from outer race defect. It is obvious that the samples from outer race defect and inner race defect are distributed in lines, which imply the influences of phase differences are not completely eliminated by TFDM method.

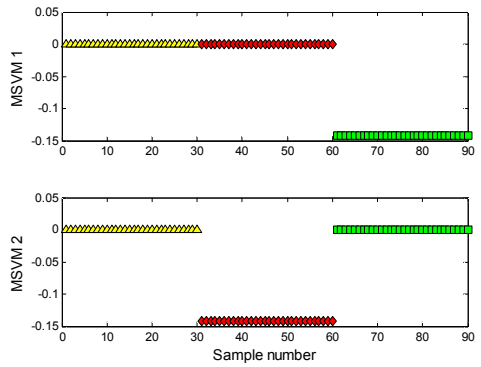

(a)

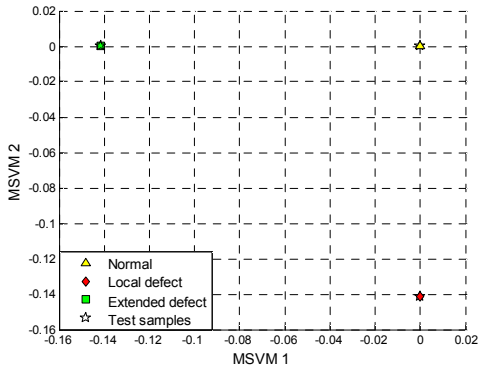

(b)

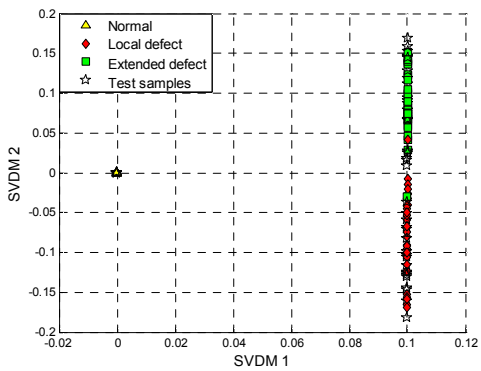

(c)

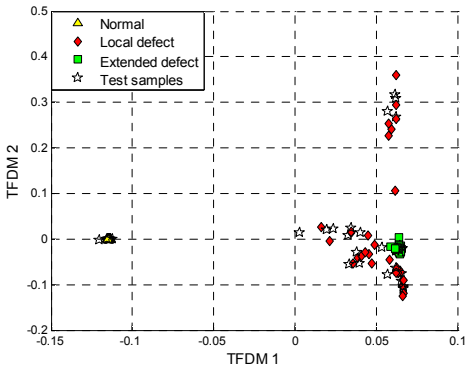

(d)

Fig. 9. Clustering results: (a) MSVM features; (b) MSVM; (c) SVDM; (d) TFDM.

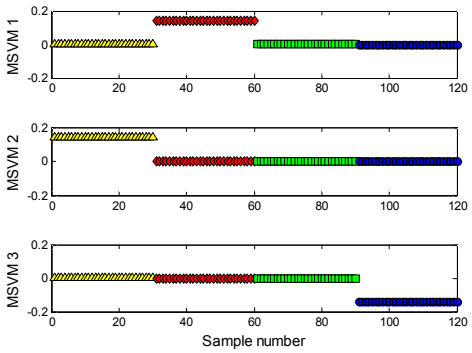

(a)

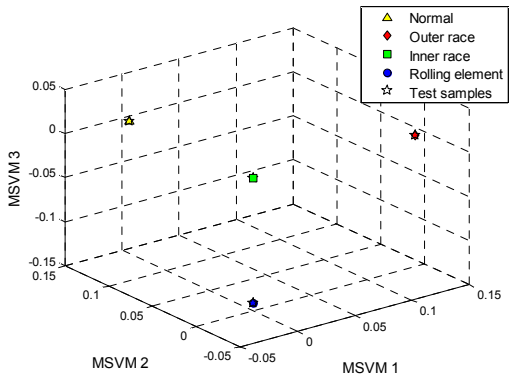

(b)

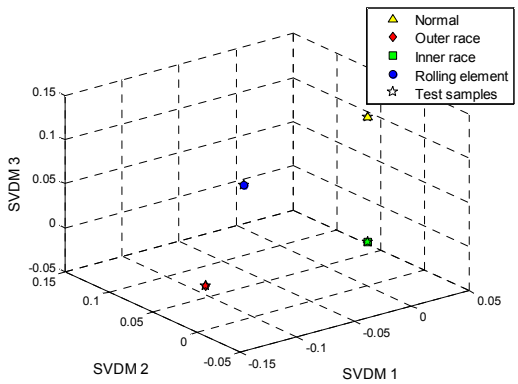

(c)

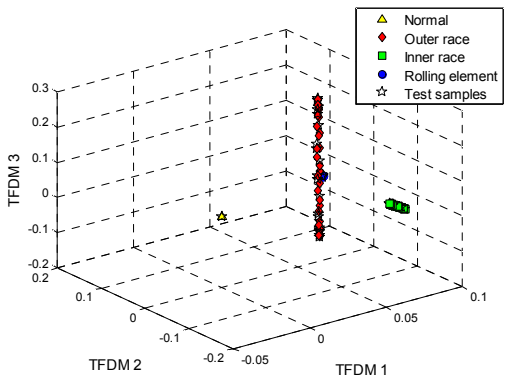

(d)

Fig. 10. Clustering results: (a) MSVM features; (b) MSVM; (c) SVDM; (d) TFDM.

Table 4. Concentration degrees and classification accuracies.

Method	Concentration degree				Total classification accuracy				Effective cases
	Case I	Case II	Case III	Case IV	Case I	Case II	Case III	Case IV	
MSVM	1.55×10^{12}	2.05×10^{11}	1.97×10^{10}	1.23×10^{10}	100 %	100 %	100 %	100 %	4
SVDM	5.0762	5.5046	1.02×10^{8}	2.53×10^{9}	95 %	93.33 %	100 %	100 %	2
TFDM	1.3865	3.4102	3.4523	4.1429	88.33 %	96.67 %	100 %	40 %	1

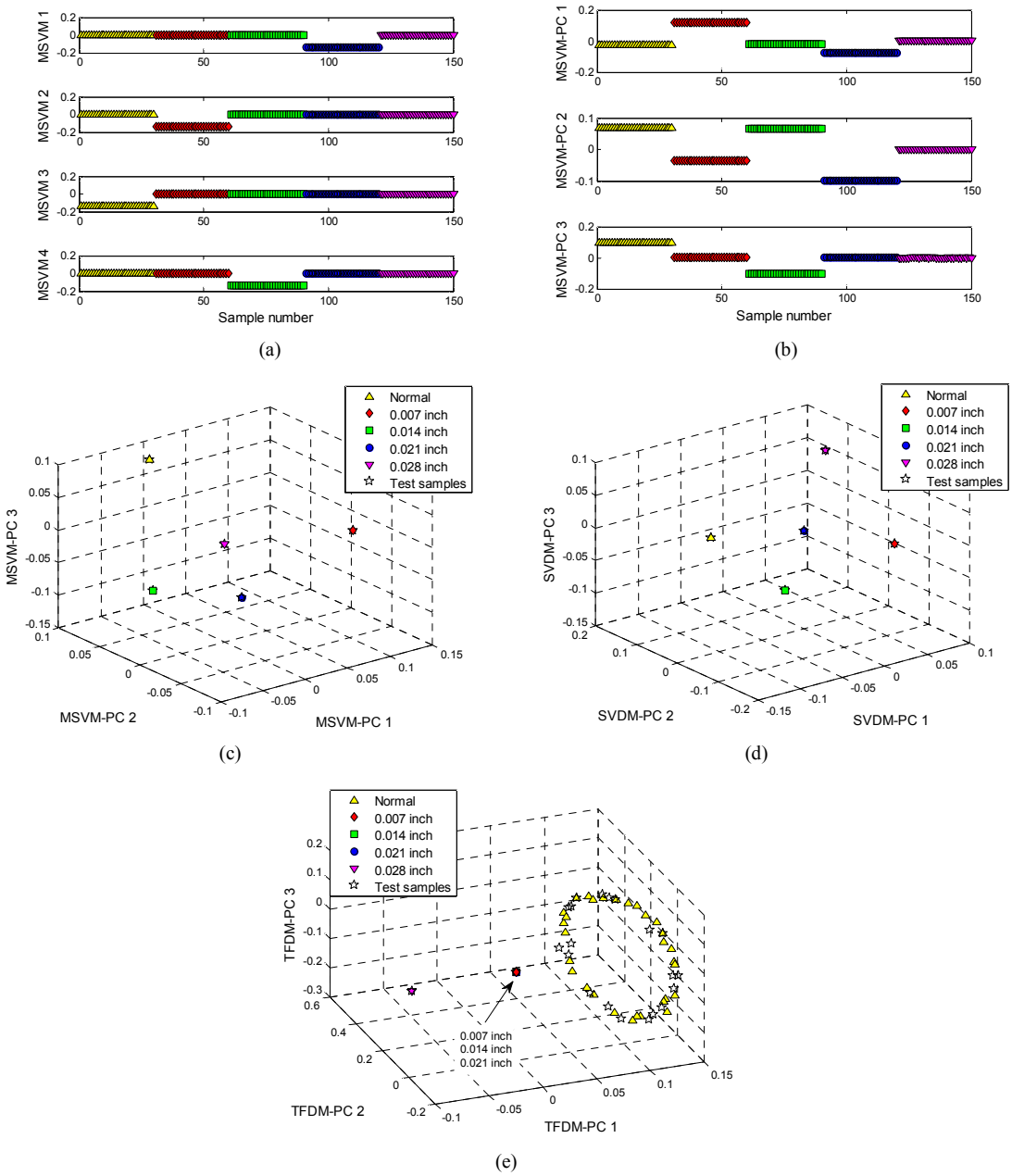

Fig. 11. Clustering results: (a) MSVM features; (b) MSVM-PC feature; (c) MSVM-PC; (d) SVDM-PC; (e) TFDM-PC.

Case IV: Multiple fault severities

Vibration signal samples of fault bearings with different defect sizes are also collected from the CWRU bearing data center. The defects are artificially machined on the surfaces of inner race with defect sizes 0.007, 0.014, 0.021 and 0.028 inch. The rotating frequency of drive shaft is 30 Hz, the sampling frequency is 12000 Hz and the sampling time of each signal sample is 0.4 second.

The dimensionality reduction parameter d is set to be 4. To show the low-dimensional features in 3-dimension, the dimen-

sions of MSVM, SVDM and TFDM features are reduced to three by PCA. As the low-dimensional features and the clustering results show in Figs. 11(a)-(d), all samples are almost distributed at five points and the sample concentrating effect of SVDM method is consistent with that of MSVM method. As the image recognition results of TFDM show in Fig. 11(e), only normal samples and the fault samples from defect size 0.028 inch are distinguished, while the remaining fault samples from the other three defect sizes are almost distributed at the same point and these fault samples are unrecognizable. It can be observed that the normal samples are distributed on a circle, which is caused by the phase differences of rotating frequency modulation.

4. Quantitative analysis

To determine the concentration degree of samples, a quantitative variable C (the ratio of mean distance among sample centers of different classes and mean distance of samples to the corresponding class center, a larger C means the samples from different classes are easier to distinguish) is defined as:

$$C = \frac{q\sum_{k=1}^{p}\sum_{l=1}^{p}\left|\overline{s}^{k} - \overline{s}^{l}\right|}{(p-1)\sum_{i=1}^{p}\sum_{j=1}^{q}\left|\overline{s}^{i} - s_{j}^{i}\right|}. \quad (17)$$

In p classes of signal samples, each class contains q samples, where s_j^i is the j-th sample which belongs to the i-th class, $\overline{s}^i$ is the sample center of the i-th class.

The concentration degree C and the classification result of each case are shown in Table 4. In all of four cases, the concentration degrees of MSVM method are the highest and the corresponding classification accuracies are 100 %, which indicates that the performance of MSVM method in sample clustering is the best and MSVM method can distinguish sample classes from each other and recognize fault patterns accurately.

Note that the SVDM method can also accurately recognize each signal class in cases III and IV, while its performance is not quite stable in cases I and II. In case III the defect positions are different, which means the fault feature frequencies and the time spacing of transient impulses are different. Such significant differences can be effectively reflected in time domain and extracted by SVD. In case IV the defect sizes on inner race are different, while the defect types are still single and local style. The durations and amplitudes of transient impulses would be changed by different sizes of local defects. Such typical changes can be also reflected in time domain and extracted by SVD.

However, defect types are diverse. As the gearbox signals show in Fig. 5, the TFDs of normal signal and pitting defect signal are very similar and there are meshing signal components with similar time spacing in both of them. Compared to the signals in time domain in Fig. 12(a), more differences in details are clearly expressed in time-frequency domain, which cannot be completely reflected in time domain. Therefore, the samples from normal and pitting defect are not accurately identified by the SVD method based on time domain.

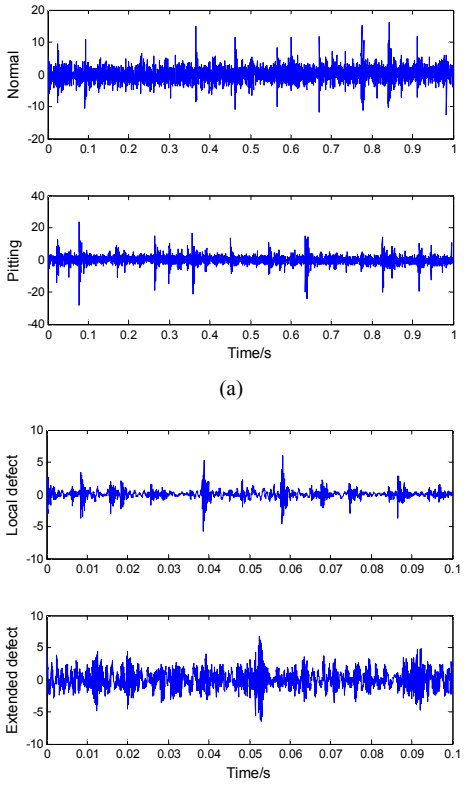

Fig. 12. Signals in time domain: (a) Normal and pitting signals of gearbox; (b) local defect and extended defect signals of bearings.

Moreover, as the TFDs of case II shown in Fig. 8, the center frequency and amplitude of transient impulses in TFDs of local defect and extended defect signals are the same. Since the defective range of bearing with extended defect is larger, rolling elements would always contact with defects and then some successive and abnormal components generate. These successive and abnormal components are similar to noise, as shown in Fig. 12(b). The results of SVD method are interfered by these noise-like components. Therefore, the samples from local defect and extended defect are not accurately identified by SVD method.

The characteristics of signals in time domain cannot comprehensively reveal the differences between similar fault patterns. There are still some shortcomings in SVDM method since the limitations of isolated time domain characteristics.

TFDM is an image recognition method. Even though TFD samples belong to the same fault pattern, the phases of rotating frequency modulation and transient impulses are still different, as shown in Fig. 13 (red dotted lines). A TFD image can be considered as a point in $\lambda \times N$-dimension space and the corresponding points of similar images are close to each other. However, the phase differences of different TFDs would

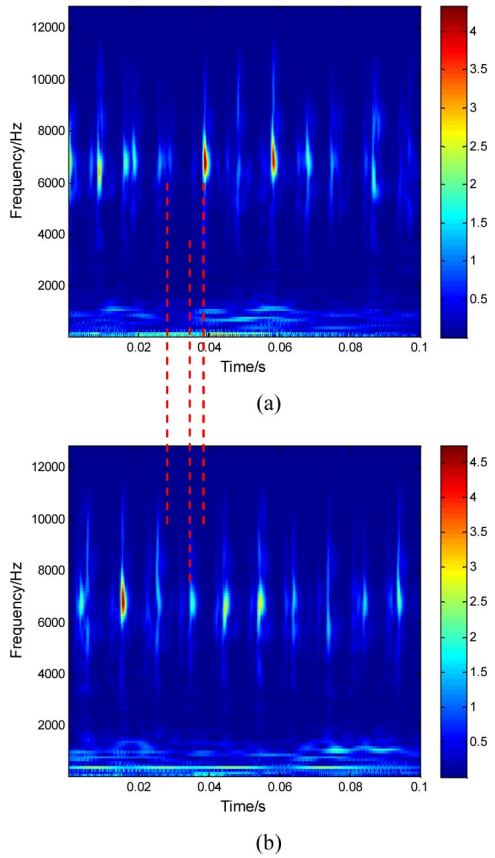

Fig. 13. Signal samples in case II: (a) Signal sample 1 with local defect; (b) signal sample 2 with local defect.

change the positional relationships of corresponding points in the space. Even though the dimension of TFDs is reduced, the TFDs from the same fault pattern are still dispersedly distributed with the lowest concentration degree.

In case II, there is no cyclical transient impulse in normal signals and the corresponding TFDs are completely different from fault signals within the frequency band 3000-10000 Hz, as shown in Fig. 8. Therefore, the corresponding points of normal samples are away from the fault samples and normal pattern can be easily distinguished from fault patterns.

In case III, since fault patterns are completely different, the manifold structure of each pattern is far away from the others in high-dimensional space. In this particular case, the TFDs from four classes are correctly distinguished without phase difference elimination process. However, TFDM method doesn't work in cases I, II and IV when fault patterns are similar.

Consequently, SVDM is a method based on signal in time domain and there are still some limitations in multi-fault pattern recognition; the image recognition method TFDM cannot recognize similar fault patterns. MSVM method can eliminate the effects of phase differences and extract the inherent features of TFDs. The performance of MSVM method is superior and stable in multi-fault pattern recognition.

5. Conclusions

We have proposed a novel multiscale singular value manifold method based on image recognition for rotating machinery fault diagnosis. To achieve image recognition, signal samples must be previously converted to images; thus continuous wavelet transform is applied to represent the time-frequency distribution images of vibration signals. Since the phase differences of transient impulses in different TFDs are obstacles to image recognition, phase space reconstruction and singular value decomposition are applied to eliminate the influences of phase differences and extract the inherent features of TFDs. Taking into account the nonlinear characteristics of high-dimensional features, manifold learning is applied to reduce the dimension of nonlinear multiscale singular value vectors of samples, and then the low-dimensional MSVM features of samples are obtained which are beneficial to pattern recognition and fault diagnosis. Comparison verifications indicate that multiscale singular value manifold method exhibits excellent stability and applicability. Experimental results prove that the proposed method can extract the features of time-frequency distribution images of vibration signals, and the low-dimensional MSVM features can recognize fault patterns of signal samples accurately and effectively.

Acknowledgment

This work is supported by the National Natural Science Foundation of China (Nos. 51275245 and 61374133).

References

[1] J. K. Hammond and P. R. White, The analysis of non-stationary signals using time–frequency methods, *J. of Sound and Vibration*, 190 (3) (1996) 419-447.

[2] E. Sejdic, I. Djurovic and J. Jiang, Time–frequency feature representation using energy concentration: an overview of recent advances, *Digital Signal Processing*, 19 (1) (2009) 153-183.

[3] J. B. Tenenbaum, V. de Silva and J. C. Langford, A global geometric framework for nonlinear dimensionality reduction, *Science*, 290 (5500) (2000) 2319-2323.

[4] S. T. Roweis and L. K. Saul, Nonlinear dimensionality reduction by locally linear embedding, *Science*, 290 (5500) (2000) 2323-2326.

[5] K. Q. Weinberger and L. K. Saul, Unsupervised learning of image manifolds by semidefinite programming, *International J. of Computer Vision*, 70 (1) (2006) 77-90.

[6] S. Kadoury and M. D. Levine, Face detection in gray scale images using locally linear embeddings, *Computer Vison and Image Understanding*, 105 (1) (2007) 1-20.

[7] Z. Y Zhang and H. Y Zha, Principal manifolds and nonlinear dimensionality reduction via tangent space alignment, *SIAM J. on Scientific Computing*, 26 (1) (2004) 313-338.

[8] Y. Zhang, B. W Li and W. Wang, Supervised locally tangent

space alignment for machine fault diagnosis, *J. of Mechanical Science and Technology*, 28 (8) (2014) 2971-2977.
[9] J. Wang, Q. B. He and F. R. Kong, Multiscale envelope manifold for enhanced fault diagnosis of rotating machines, *Mechanical Systems and Signal Processing*, 52-53 (2015) 376-392.
[10] Q. He, Y. Liu, Q. Long and J. Wang, Time-frequency manifold as a signature for machine health diagnosis, *IEEE Transactions on Instrumentation and Measurement*, 61 (5) (2012) 1218-1230.
[11] Z. Q Su, B. P. Tang, Z. R Liu and Y. Qin, Multi-fault diagnosis for rotating machinery based on orthogonal supervised linear local tangent space alignment and least square support vector machine, *Neurocomputing*, 157 (2015) 208-222.
[12] M. Gan, C. Wang and C. A. Zhu, Multiple-domain manifold for feature extraction in machinery fault diagnosis, *Measurement,* 75 (2015) 76-91.
[13] N. E. Huang, Z. Shen and S. R. Long, The empirical mode decomposition and Hilbert spectrum for nonlinear and non-stationary time series analysis, *Proceedings of the Royal Society of London, Series A-Mathematical Physical and Engineering Sciences*, 454 (1998) 903-995.
[14] J. Lin and L. S. Qu, Feature extraction based on Morlet wavelet and its application for mechanical fault diagnosis, *J. of Sound and Vibration*, 234 (1) (2000)135-148.
[15] Y. T. Sheen and C. K. Hung, Constructing a wavelet-based envelope function for vibration signal analysis, *Mechanical Systems and Signal Processing*, 18 (1) (2004) 119-126.
[16] G. P. King and I. Stewart, Phase-space reconstruction for symmetrical dynamic-systems, *Physica D*, 58 (1-4) (1992) 216-228.
[17] L. Cao, Practical method for determining the minimum embedding dimension of a scalar time series, *Physica D*, 110 (1/2) (1997) 43-50.
[18] F. Takens, Detecting strange attractors in turbulence, *Dynamical System and Turbulence*, 898 (1981) 366-387.
[19] M. Bydder and J. Du, Noise reduction in multiple-echo data sets using singular value decomposition, *Magnetic Resonance Imaging*, 24 (7) (2006) 849-856.
[20] A. Widodo and B. S. Yang, Support vector machine in machine condition monitoring and fault diagnosis, *Mechanical Systems and Signal Processing*, 21 (2007) 2560-2574.
[21] C. W. Hsu and C. J. Lin, A comparison of methods for multiclass support vector machines, *IEEE Transactions on Neural Networks*, 13 (2) (2002) 415-425.
[22] G. M. Lim, D. M. Bae and J. H. Kim, Fault diagnosis of rotating machine by thermography method on support vector machine, *J. of Mechanical Science and Technology*, 28 (8) (2014) 2947-2952.
[23] *http://csegroups.case.edu/bearingdatacenter/pages/download-data-file.*

Yi Feng received his B.S. from Nanjing University of Science and Technology, Nanjing, China, in 2012. He is currently working toward the Ph.D. in Mechanical Engineering. His research interests include signal processing and fault diagnosis.

Baochun Lu received his Ph.D. from Nanjing University of Science and Technology, Nanjing, China, in 2002. He currently works at Nanjing University of Science and Technology. His research interests include mechanical engineering automation and fault diagnosis.

Dengfeng Zhang received his Ph.D. from Nanjing University of Science and Technology, Nanjing, China, in 2003. He currently works at Nanjing University of Science and Technology. His research interests include fault tolerant control.